Published OnlineFirst February 1, 2017; DOI: 10.1158/1535-7163.MCT-16-0496

Small Molecule Therapeutics

Molecular Cancer Therapeutics

Clinical Dosing Regimen of Selinexor Maintains Normal Immune Homeostasis and T-cell Effector Function in Mice: Implications for Combination with Immunotherapy

Paul M. Tyler[1], Mariah M. Servos[1], Romy C. de Vries[1,2], Boris Klebanov[3], Trinayan Kashyap[3], Sharon Sacham[3], Yosef Landesman[3], Michael Dougan[4], and Stephanie K. Dougan[1]

Abstract

Selinexor (KPT-330) is a first-in-class nuclear transport inhibitor currently in clinical trials as an anticancer agent. To determine how selinexor might affect antitumor immunity, we analyzed immune homeostasis in mice treated with selinexor and found disruptions in T-cell development, a progressive loss of CD8 T cells, and increases in inflammatory monocytes. Antibody production in response to immunization was mostly normal. Precursor populations in bone marrow and thymus were unaffected by selinexor, suggesting that normal immune homeostasis could recover. We found that a high dose of selinexor given once per week preserved nearly normal immune functioning, whereas a lower dose given 3 times per week did not restore immune homeostasis. Both naïve and effector CD8 T cells cultured *in vitro* showed impaired activation in the presence of selinexor. These experiments suggest that nuclear exportins are required for T-cell development and function. We determined the minimum concentration of selinexor required to block T-cell activation and showed that T-cell–inhibitory effects of selinexor occur at levels above 100 nmol/L, corresponding to the first 24 hours post-oral dosing. In a model of implantable melanoma, selinexor treatment at 10 mg/kg with a 4-day drug holiday led to intratumoral IFNγ$^+$, granzyme B$^+$ cytotoxic CD8 T cells that were comparable with vehicle-treated mice. Overall, selinexor treatment leads to transient inhibition of T-cell activation, but clinically relevant once and twice weekly dosing schedules that incorporate sufficient drug holidays allow for normal CD8 T-cell functioning and development of antitumor immunity. *Mol Cancer Ther; 16(3); 428–39. ©2017 AACR.*

See related article by Farren et al., p. 417

Introduction

Tumor suppressor proteins, such as p53, play a key role in genome integrity and, as such, are frequently mutated in many types of malignancies (1). However, many cancers effectively inactivate p53 and other tumor suppressors by upregulation of the exportin XPO1, which shuttles p53 out of the nucleus (2). XPO1 belongs to a family of proteins called karyopherins, which regulate nuclear transport (3). Importins bind to nuclear localization sequences on cargo proteins and translocate to the nucleus, where binding of Ran-GTP allows for dissociation of the cargo and recycling of importin to the cytosol. Conversely, exportins, such as XPO1, bind Ran-GTP and nuclear export sequences on cargo proteins inside the nucleus and are transported out of the nucleus (3–5). XPO1 facilitates the transport of approximately 200 cargo proteins, including the tumor suppressor proteins p53, BRCA, IκB, p21, and FOXO (6). XPO1 also shuttles eukaryotic initiation factor 4e (eIF4e), which transports guanine-capped mRNAs, including those encoding key oncogenes, into the cytosol (7). Enhanced XPO1 activity results in the removal of p53 from the nucleus and increased transcript levels of myc, cyclin D1, and MDM2 (7). XPO1 is overexpressed or correlates with poor prognosis in many tumor types, including glioma, osteosarcoma, pancreatic, gastric, ovarian, and cervical cancers, highlighting the importance of nuclear transport to maintaining the nontransformed state (8–14).

Selective inhibitors of nuclear export compounds have been developed. Selinexor (KPT-330) is a highly specific, slowly reversible, covalent inhibitor of XPO1 and has shown promising results in phase I/II clinical trials of hematologic and solid malignancies (15–17). Selinexor treatment dramatically reduces tumor burden in a variety of both xenograft and syngeneic mouse models (18–23). Although selinexor is fairly well tolerated, side effects of treatment include fatigue, nausea, and thrombocytopenia (17).

Selinexor traps all XPO1 target proteins in the nucleus, which includes several transcription factors or transcription factor regulators that play critical roles in immune system function: NFATc1, IκBα, p100, and p65 (subunits of NF-κB), cIAP1, STAT1, and STAT3 (6). Although transcription factors bind DNA in the nucleus, many transcription factors require dimerization,

[1]Dana-Farber Cancer Institute, Boston, Massachusetts. [2]University of Amsterdam, Program in Biomedical Sciences, Amsterdam, the Netherlands. [3]Karyopharm Therapeutics, Inc., Newton, Massachusetts. [4]Massachusetts General Hospital, Boston, Massachusetts.

Note: Supplementary data for this article are available at Molecular Cancer Therapeutics Online (http://mct.aacrjournals.org/).

P.M. Tyler and M.M. Servos contributed equally to this article.

Corresponding Author: Stephanie K. Dougan, Dana-Farber Cancer Institute, 450 Brookline Ave., Smith 770A, Boston, MA 02215. Phone: 617-582-9609; Fax: 617-582-9610; E-mail: Stephanie_Dougan@dfci.harvard.edu

doi: 10.1158/1535-7163.MCT-16-0496

Published OnlineFirst February 1, 2017; DOI: 10.1158/1535-7163.MCT-16-0496

phosphorylation, ligand binding, or proteolytic degradation of an inhibitory protein for their activity. Many of these events occur in the cytosol; thus, inhibition of XPO1 can constitutively trap transcription factors in either active or inactive forms. STAT1 activity is transiently enhanced by nuclear localization, but inhibition of nuclear export of STAT1 results in diminished ability of cells to upregulate transcription of IFNγ-responsive genes (24). STAT3 is transported to the nucleus in its inactive conformation in noncytokine-stimulated cells, and addition of the XPO1 inhibitor leptomycin B leads to the accumulation of inactive STAT3 in the nucleus (25). NF-κB becomes trapped in the nucleus along with its inhibitor IκBα, leading to abrogation of activity upon treatment with selinexor or leptomycin B (5, 26–28). Other proteins of immunologic interest that rely on XPO1 for nuclear export include fyn, AID, AHR, and DGKζ, although it is unclear how loss of XPO1 function would affect the activity of these targets (21).

The immune system is important for both controlling infection and in the generation of antitumor immunity. Cytotoxic T cells, in particular, correlate with increased overall survival in colorectal and other cancers (29). Immunotherapy has shown impressive clinical benefit, particularly for metastatic melanoma. The FDA has approved four immune-modulating drugs that target T-cell–inhibitory pathways, ipilimumab (anti-CTLA-4), nivolumab/pembrolizumab (anti-PD-1), and atezolizumab (anti-PD-L1; refs. 30–33). As immunotherapy targets the immune system, and not a particular type of cancer, these new drugs were originally hoped to be applicable across all tumor types as a pan-cancer medication. Indeed, significant clinical results have been seen for ipilimumab or PD-1 blockade in non–small cell lung cancer, renal cell cancer, castration-resistant prostate cancer, Hodgkin lymphoma, and multiple cancer types deficient in mismatch repair (31, 32, 34, 35). The clinical success of mAbs targeting negative regulators on T cells demonstrates that a significant fraction of cancer patients have antitumor T cells at baseline and that manipulating these T cells can have therapeutic benefit.

Naïve tumor-specific T cells must be primed by dendritic cells presenting antigens released from dying tumor cells. This priming stage is necessary for the expansion of tumor-specific clones and for the acquisition of effector functions, such as cytotoxicity and cytokine production. T-cell priming is enhanced by dying tumor cells, which release both antigens and endogenous danger signals, such as HMGB1 or 2′3′cGAMP, which can activate dendritic cells to enhance antigen presentation, expression of costimulatory molecules, and trafficking to the tumor-draining lymph node (36, 37). Therapies that kill tumor cells would be predicted to enhance T-cell priming and synergize with immunotherapy, and indeed, this has been the case for radiation (38, 39), chemotherapy (36, 40), and some targeted therapies (41, 42).

The general ability of most conventional therapies to enhance response to immunotherapy has led to a flurry of combination clinical trials. Immunotherapy has the potential for durable long-term remissions; however, the fraction of patients who respond is relatively low for most cancer types. Combination therapy is likely necessary to extend the benefit of immunotherapy to more patients. Although general consensus and support for combination therapy exists, most standard cancer therapies have not been evaluated for their effects on the immune system, or those effects have been equivocal. For example, radiation releases tumor antigens (39), but also stimulates radiation-resistant mesenchymal stem cells, which can cause local immunosuppression and make irradiated bone marrow a preferred metastatic niche (43). Chemotherapies kill rapidly dividing cells, with certain agents preferentially eliminating regulatory T cells (Treg; ref. 44), myeloid-derived suppressor cells (MDSC; refs. 45, 46), or even proliferating CD8 T cells (47). A better understanding of the effects of various cancer treatments on cells of the immune system is important for making rationally designed combination strategies.

Here, we examined the effects of selinexor on normal immune homeostasis in mice and recapitulated a side effect profile similar to that seen in humans. We further showed that naïve and effector CD8 T cells were inhibited by selinexor, but only at high concentrations and for a short time window. We show that decreased frequency of selinexor dosing greatly mitigates these effects, and we successfully predicted a regimen of selinexor dosing that allows for simultaneous development of robust antitumor immunity. These findings illustrate a simple preclinical method for assessing novel chemotherapies in combination with immunotherapy using established murine models.

Materials and Methods

Animal care

All animals were housed at Dana-Farber Cancer Institute (Boston, MA) and were maintained according to protocols approved by the DFCI IACUC Committee on Animal Care. C57BL/6 and OT-I;RAG1$^{-/-}$ mice were purchased from The Jackson Laboratory. TRP1^{high};CD45.1 mice were bred in-house (48).

Reagents

Selinexor was dissolved in DMSO for use in *in vitro* assays. For *in vivo* studies, selinexor was diluted to 1.5 mg/mL in water with 0.6% w/v Pluronic F-68 and 0.6% w/v PVP K-29/32.

Immunizations

C57BL/6 mice were immunized with 100 μg ovalbumin (Sigma) dissolved in 100 μL PBS per mouse and mixed 1:1 with complete Freund adjuvant (Sigma). Each mouse received 200 μL immunogen mixture intraperitoneally. Mice were boosted on day 14 postimmunization, with 100 μg ovalbumin mixed 1:1 with incomplete Freund adjuvant (Sigma). Mice were bled at days 7, 14, 21, and 28 postimmunization. Blood was permitted to clot and then centrifuged at 1,100 × *g* for 5 minutes to obtain serum. Serum samples were diluted at the indicated dilution factors and analyzed by ELISA using ovalbumin-coated plates and secondary anti-mouse Igκ coupled to HRP (SouthernBiotech).

Flow cytometry

Cells were harvested from spleen, mesenteric lymph nodes, bone marrow, or thymus. Tissues were crushed into PBS through a 40-μm cell strainer using the back of a 1-mL syringe plunger. Cell preparations were subjected to hypotonic lysis to remove erythrocytes, stained and analyzed using a Fortessa (BD Biosciences). CD1d(PBS57) tetramer was obtained from the NIH Tetramer Core Facility. Flow cytometry antibodies used in this study were purchased from BioLegend [anti-B220-PacificBlue (clone RA3-6B2), anti-CD107a-Fitc (1D4B), anti-CD11b-AlexaFluorophore 488 (M1/70), anti-CD11c-APC (N418), anti-CD11c-PE/Cy7 (N418), anti-CD25-AlexaFluorophore 488 (PC61), anti-CD44-Bv421 (IM7), anti-CD44-PE/Cy7 (IM7), anti-CD45-Bv711 (30-F11), anti-CD45.1-Bv711 (A20), anti-CD4-APC (RM4-5), anti-CD4-PacificBlue (RM4-5), anti-CD69-PE (H1.2F3), anti-

Published OnlineFirst February 1, 2017; DOI: 10.1158/1535-7163.MCT-16-0496

CD8-Bv650 (53-6.7), anti-FoxP3-PE (MF-14), anti-Gr1-PE (RB6-8C5), anti-Gr1-PE/Cy7 (RB6-8C5), anti-IFNγ-Bv421 (XMG1.2), anti-LAG3-Pe (C9B7W), anti-MHC I-A/I-E-Bv510 (M5/114.15.2), anti-NK1.1-FITC (PK136), anti-NK1.1-PE/Cy7 (PK136), anti-PD-1-PE/Cy7 (29F.1A12), and Tim3-APC (RMT3-23)] and Affymetrix [anti-CD19-PE (MB19-1) and anti-GrzB-Pe/Cy7 (NGZB)].

Cell culturing

Cells were cultured in RPMI1640 medium supplemented with 10% heat-inactivated FBS, 2 mmol/L L-glutamine, 100 U/mL penicillin G sodium, 100 μg/mL streptomycin sulfate, 1 mmol/L sodium pyruvate, 0.1 mmol/L nonessential amino acids, and 0.1 mmol/L 2-ME. CD8 T cells were isolated from pooled spleen and lymph nodes of TRP1^{high};CD45.1, OT-I:RAG1$^{-/-}$ or wild-type mice using positive selection on anti-CD8 magnetic beads (Dynabeads, Invitrogen). For generation of effector CD8 T cells, isolated naïve CD8 T cells were plated into 12-well dishes at 1×10^6 cells per mL with anti-CD3/CD28 beads (Invitrogen) and 100 U/mL recombinant human IL2 (Peprotech). Beads were removed after 48 hours, and fresh IL2-containing media were added every 2 to 3 days. T cells were cultured for 7 days prior to washing, counting, and plating into 24-well dishes containing B16 cells or B16 that had been transduced with ovalbumin (B16OVA) cells that had been pretreated for 24 hours with recombinant mouse IFNγ (10 ng/mL; Peprotech) to induce upregulation of surface MHC class I. A total of 2×10^5 T cells were added per well.

Naïve T-cell activation assays

CD8 T cells were isolated using positive selection as described above. They were plated in triplicate at a final concentration of 1×10^5 cells/200 μL in 96-well plates containing 100 U/mL recombinant IL2 and either B cells presenting an appropriate peptide (TRP1 or SIINFEKL), anti-CD3/CD28 beads, or PMA/ionomycin. The time points at which selinexor was added and the concentrations of peptide used varied and are described in the figures. After 48 hours of culture, T cells were washed and stained for extracellular and intracellular markers of activation.

Intracellular cytokine staining

Cells were cultured in the presence of GolgiStop (BD Biosciences) for 3 to 5 hours and then washed and stained with antibodies against extracellular markers, washed in PBS, and suspended in fixation buffer (BioLegend) for 20 minutes. Cells were washed twice with permeabilization wash buffer (BioLegend) and stained with antibodies against cytokines overnight. Cells were then washed in PBS and analyzed using a Fortessa.

B16 tumor inoculations and selinexor *in vivo* dosing

B16F10 (ATCC CRL6475) cells were obtained from the ATTC (February 2015) and were used within 6 months. B16 cells were screened prior to use for murine pathogens, including mycobacteria (Charles River Laboratories). No further authentication was performed by the authors. B16 cells were cultured to 90% confluency, trypsinized, washed in Hank balanced salt solution (HBSS), and resuspended in HBSS at 1×10^5 tumor cells per 250 μL volume. Cells were injected subcutaneously in the left flank of 6- to 12-week-old female C57BL/6 mice. Mice were dosed with vehicle or selinexor by oral gavage using an 18-gauge curved ball–bearing syringe tip. For adoptive transfers, unless otherwise stated, mice received 5×10^5 TRP^{high};CD45.1 CD8 T cells in 150 μL PBS administered via tail vein injection on day 7 after tumor inoculation. Selinexor was dosed at 7.5, 10, or 15 mg/kg as indicated in the figure legends. Dosing occurred 3 times per week (Monday, Wednesday, and Friday), twice per week (Monday and Wednesday), or once per week on Mondays.

Statistical analysis

Student *t* test was used to compare means. Error bars are SD throughout.

Results

Selinexor affects normal immune homeostasis, with the greatest effect on CD8 T cells

To determine the effects of selinexor on normal immune homeostasis, we treated mice orally with vehicle control or selinexor at 15 mg/kg 3 times per week (Monday, Wednesday, and Friday). Mice were treated for 1, 2, or 4 weeks, and thymus, bone marrow, and spleen populations were analyzed. A striking loss of thymus cellularity was evident (Fig. 1A) soon after start of treatment. T-cell development occurs in the thymus, with T-cell precursors arriving as CD4$^-$CD8$^-$ (double negative, DN) cells that undergo RAG-mediated recombination of their TCRβ and TCRα genes to form functional T-cell receptors (TCR; ref. 49). Once a functional TCR is expressed, T cells upregulate CD4 and CD8 to become double-positive (DP) cells. During this stage of thymic development, which can last up to 3 weeks, developing T cells must experience TCR signaling of intermediate strength, indicating that the newly formed TCR binds to peptide–MHC complexes expressed by the host, but is not overtly self-reactive (49). Selinexor interferes with this process, as shown by a pronounced loss of DP cells (Fig. 1B). T cells that do manage to survive positive and negative selection to become single-positive CD4 or CD8 T cells are not overtly killed by selinexor. Defects in thymic selection can often be most pronounced on minor populations, such as NKT cells or CD4$^+$ regulatory T cells; however, these populations were present at normal abundance after 14 and even 28 days of selinexor treatment (Fig. 1C; and data not shown). Within the DN population, all subsets were present as determined by CD25 and CD44 expression (Fig. 1D), suggesting that T-cell development proceeded normally up to the DP stage.

We next examined the bone marrow of vehicle control or 28-day selinexor-treated mice. Hematopoietic stem cells, contained within the lineage-negative fraction, were not obviously inhibited by selinexor treatment as total cellularity of the bone marrow was maintained, and most populations of cells appeared to be present. We observed a striking absence of CD8 T cells in the bone marrow, as well as an apparent block in B-cell development with more B cells stuck in the earlier pro- and pre–B-cell stages of development and fewer immature B cells in selinexor-treated mice (Fig. 1E). In the spleen, we observed a progressive loss of CD8 T cells over time, with a concomitant increase in monocytes (Fig. 1F).

Selinexor treatment only modestly affects antibody production

One of the target proteins of XPO1 is activation-induced deaminase (AID), an enzyme critical for B-cell isotype switching and affinity maturation. Without AID function, high-affinity IgGs cannot be produced. To investigate AID function in the context of selinexor treatment, we immunized mice with a model antigen ovalbumin and measured ovalbumin-specific

Published OnlineFirst February 1, 2017; DOI: 10.1158/1535-7163.MCT-16-0496

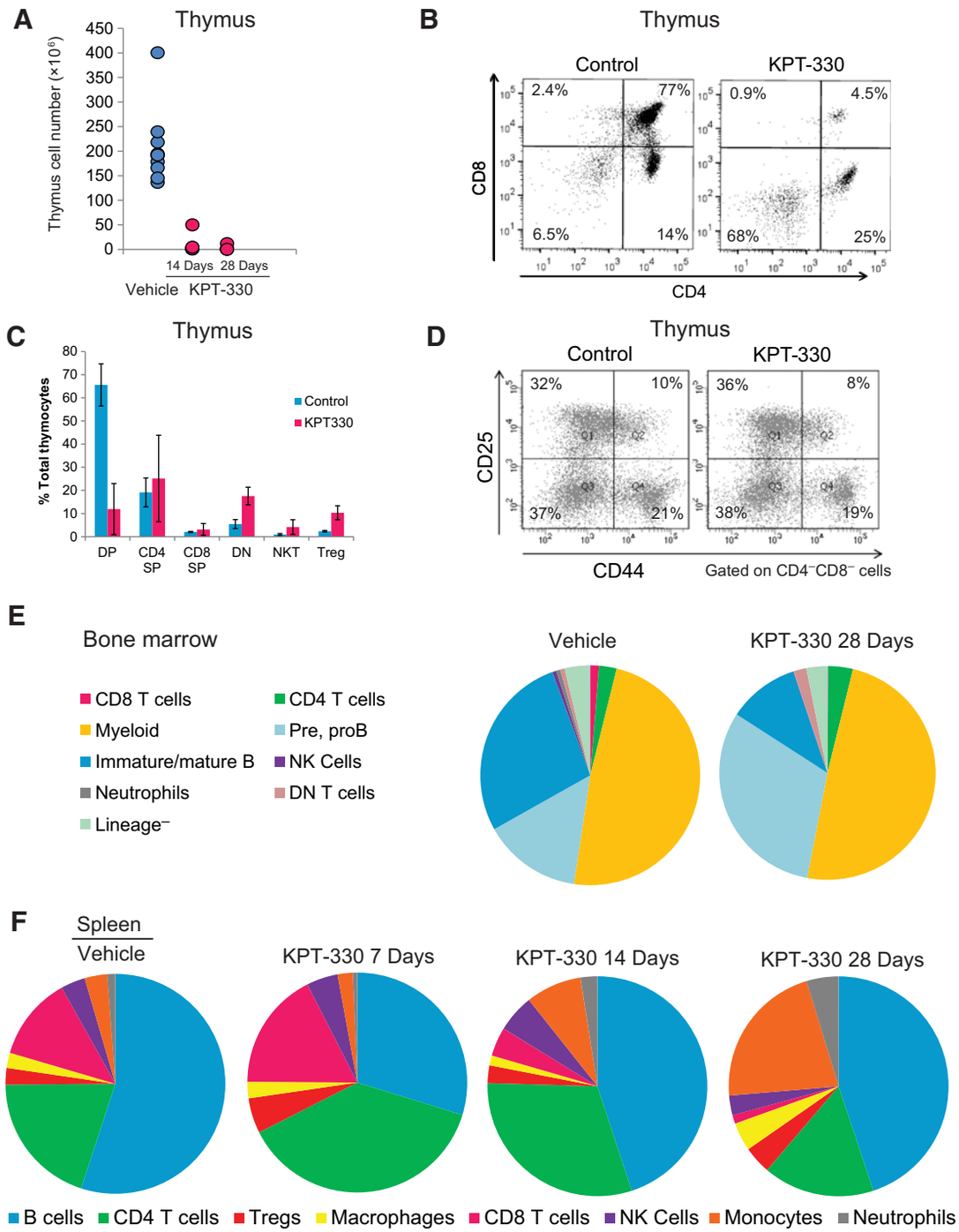

Figure 1.

Selinexor disrupts normal immune homeostasis. **A,** C57BL/6 mice were treated with vehicle or KPT-330 (15 mg/kg) by oral gavage 3 times per week (Monday, Wednesday, and Friday) for 2 or 4 weeks. Total thymocyte cell numbers are shown. $n = 10$, vehicle; $n = 5$ KPT-330 groups. **B,** Thymocytes from vehicle or 14-day treated mice in **A** were stained with antibodies to CD4 and CD8 and analyzed by flow cytometry. Representative image is shown. **C,** Quantification of thymic populations from vehicle or 14-day treated mice. **D,** Thymocytes from vehicle or 14-day treated mice in **A** were stained with antibodies to CD4, CD8, CD25, and CD44 and analyzed by flow cytometry. Representative image is shown, gated on $CD4^-CD8^-$ cells. **E,** C57BL/6 mice were treated with vehicle or KPT-330 (15 mg/kg) by oral gavage 3 times per week (Monday, Wednesday, and Friday) for 4 weeks. Bone marrow cells were harvested, stained with antibodies, and analyzed by flow cytometry. CD8 T cells = $CD45^+CD8^+$; CD4 T cells = $CD45^+CD4^+$; myeloid = $CD45^+CD11b^+Gr1^-$; pre, proB = $CD45^+B220^+IgD^-$; immature/mature B = $CD45^+B220^+IgD^+$; NK cells = $CD45^+NK1.1^+$; neutrophils = $CD45^+CD11b^+Gr1^+$; DN T cells = $CD45^+CD3^+CD4^-CD8^-$; lineage$^-$ = $CD45^+$ negative for all other markers. Pie chart shows average frequencies from $n = 5$ mice per group. **F,** C57BL/6 mice were treated with vehicle or KPT-330 (15 mg/kg) by oral gavage 3 times per week (Monday, Wednesday, and Friday) for 1, 2, or 4 weeks. Spleen cells were harvested, stained with antibodies, and analyzed by flow cytometry. B cells = $CD45^+B220^+$; CD4 T cells = $CD45^+CD4^+Foxp3^-$; Tregs = $CD45^+CD4^+Foxp3^+$; macrophages = $CD45^+CD11b^+Gr1^-$; CD8 T cells = $CD45^+CD8^+$; NK cells = $CD45^+NK1.1^+$; monocytes = $CD45^+CD11b^+Ly6C^+Gr1^-$; neutrophils = $CD45^+CD11b^+Gr1^+$. Pie charts show averages from $n = 5$ mice per group.

Published OnlineFirst February 1, 2017; DOI: 10.1158/1535-7163.MCT-16-0496

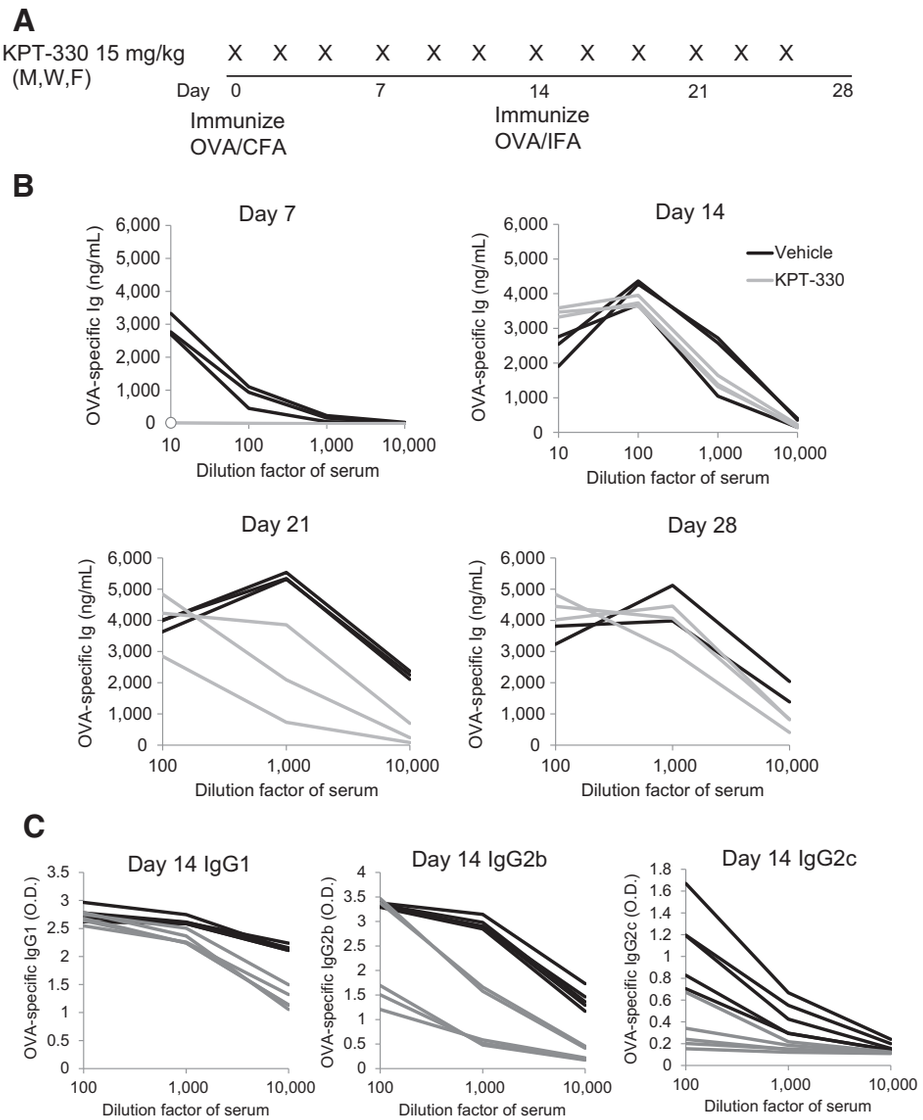

Figure 2.
Antibody production is only modestly affected by selinexor. **A,** Diagram of KPT-330 dosing and immunization schedule. M, Monday; W, Wednesday; F, Friday. **B,** C57BL/6 mice were immunized according to diagram shown in **A**. Serum was collected at the indicated time points, diluted at the indicated ratios, and used in an ELISA with ovalbumin-coated plates. Secondary anti-mouse Igκ coupled to HRP was used for detection. Each line represents one mouse. $n = 3$ mice per group. **C,** Serum was analyzed as in **B**, using secondary anti-mouse IgG1, anti-mouse IgG2b, or anti-mouse IgG2c coupled to HRP for detection.

antibody production over time (Fig. 2A). One week postimmunization, all three vehicle control–treated mice had measureable anti-ovalbumin antibodies, while the selinexor-treated mice were indistinguishable from nonimmunized controls (Fig. 2B). By 2 weeks postimmunization, this difference was no longer apparent; all selinexor mice showed high-titer anti-ovalbumin antibodies at the 2-week and later time points that were equivalent to vehicle control–treated mice. When IgG1, IgG2b, IgG2c, and IgA isotypes were analyzed, we again saw negligible differences in antigen-specific IgG1 and IgA, although mild deficiencies in antigen-specific IgG2b and IgG2c were noted. Subtle differences in affinity or clonal diversity would not be detected by the ELISA assay used. Serum IFNγ levels were similar between the two groups, as were the numbers of $CD4^+$ T follicular helper cells generated (Supplementary Fig. S1). The slight delay in antibody production could indicate a transient block in BCR signaling; this observation, combined with the block in B-cell development in the bone marrow (Fig. 1E), suggests that further study of the effects of selinexor on both malignant and normal B cells may be warranted. However, the presence of antigen-specific class-switched antibody demonstrates that AID must be functional.

Decreasing the frequency, but not the dose of selinexor, restores normal immune homeostasis

Given that the lineage-negative cells in the bone marrow, and DN populations in the thymus, were unaffected by even prolonged 28 days of selinexor treatment, we predicted that precursor populations would be intact and able to restore normal population levels in bone marrow, thymus, and secondary lymphoid organs after drug withdrawal. On the basis of preclinical assessment in a variety of tumor models, 15 mg/kg dosed 3 times per week is a relatively high dose of selinexor, and antitumor function is still observed at doses as low as 6 mg/kg (data not shown). We therefore investigated immune populations in mice dosed for 4 weeks according to the schedule shown in Fig. 3A. The 15 × 3 group received exactly the same dose regimen as the mice shown in Fig. 1, and again, we found profound loss of thymic cellularity, loss of CD8 T cells and immature B cells

Published OnlineFirst February 1, 2017; DOI: 10.1158/1535-7163.MCT-16-0496

A

Group name	Treatment	Schedule		
Vehicle	Vehicle	M	W	F
15×3	KPT-330 15 mg/kg	M	W	F
15×1	KPT-330 15 mg/kg	M		
7.5×3	KPT-330 7.5 mg/kg	M	W	F

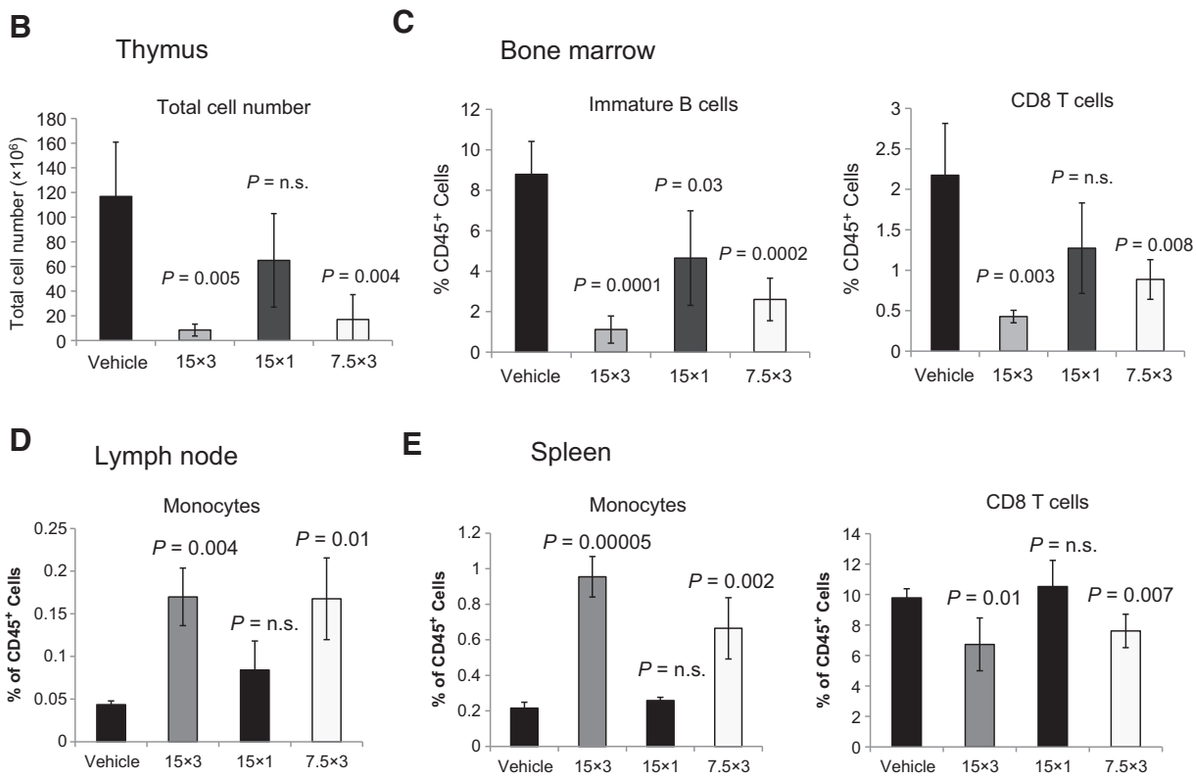

Figure 3.

Decreased frequency of selinexor treatment restores immune homeostasis better than decreased dose. **A,** C57BL/6 mice were dosed for 3 weeks according to the indicated schedules. $n = 5$ mice per group. M, Monday; W, Wednesday; F, Friday. **B,** Total thymocyte cell numbers. **C,** Bone marrow cells were harvested and stained as in Fig. 1E. CD8 T cells and immature B cells were quantified. **D,** Mesenteric lymph node cells were harvested and stained as in Fig. 1F. Monocytes were quantified. **E,** Spleen cells were harvested and stained as in Fig. 1F. Monocytes and CD8 T cells were quantified.

from the bone marrow, and loss of CD8 T cells and compensatory increases in inflammatory monocytes in the secondary lymphoid organs (Fig. 3B–E).

Our two experimental groups were mice that received one high dose of selinexor (15 × 1) versus mice that received a low dose of selinexor 3 times per week (7.5 × 3). As clearly evident, mice in the 15 × 1 group were similar to the vehicle controls, whereas mice in the 7.5 × 3 group were indistinguishable from the 15 × 3 group (Fig. 3B–E). These data demonstrate that decreasing the frequency of selinexor dosing has a much more favorable impact on immune homeostasis than decreasing the actual dose given.

Selinexor blocks TCR signaling in naïve T cells

Of all of the populations examined, CD8 T cells were most sensitive to selinexor treatment (Figs. 1 and 3). Given the importance of CD8 T cells to antitumor immunity, we wanted to examine the effects of selinexor on CD8 T-cell function in more detail. Naïve CD8 T cells were isolated from an OT-I transgenic mouse whose T cells recognize a peptide sequence from ovalbumin (SIINFEKL) presented on the MHC class I molecule H-2K^b (50). We cultured OT-I T cells with SIINFEKL pulsed antigen-presenting cells and measured T-cell proliferation by CellTrace violet dye dilution. While vehicle-treated OT-I cells proliferated in a dose-dependent fashion based on the amount of SIINFEKL peptide present, selinexor-treated OT-I cells were completely refractory to proliferation at all concentrations of antigen tested (Fig. 4A). This selinexor-induced block in CD8 T-cell activation could not be overcome by using anti-CD3/CD28–coated beads, nor through bypassing proximal TCR signaling using phorbol myristate acetate and a calcium ionophore (PMA/Ion, Fig. 4B). IFNγ production was also blocked by selinexor (Supplementary Fig. S2).

Published OnlineFirst February 1, 2017; DOI: 10.1158/1535-7163.MCT-16-0496

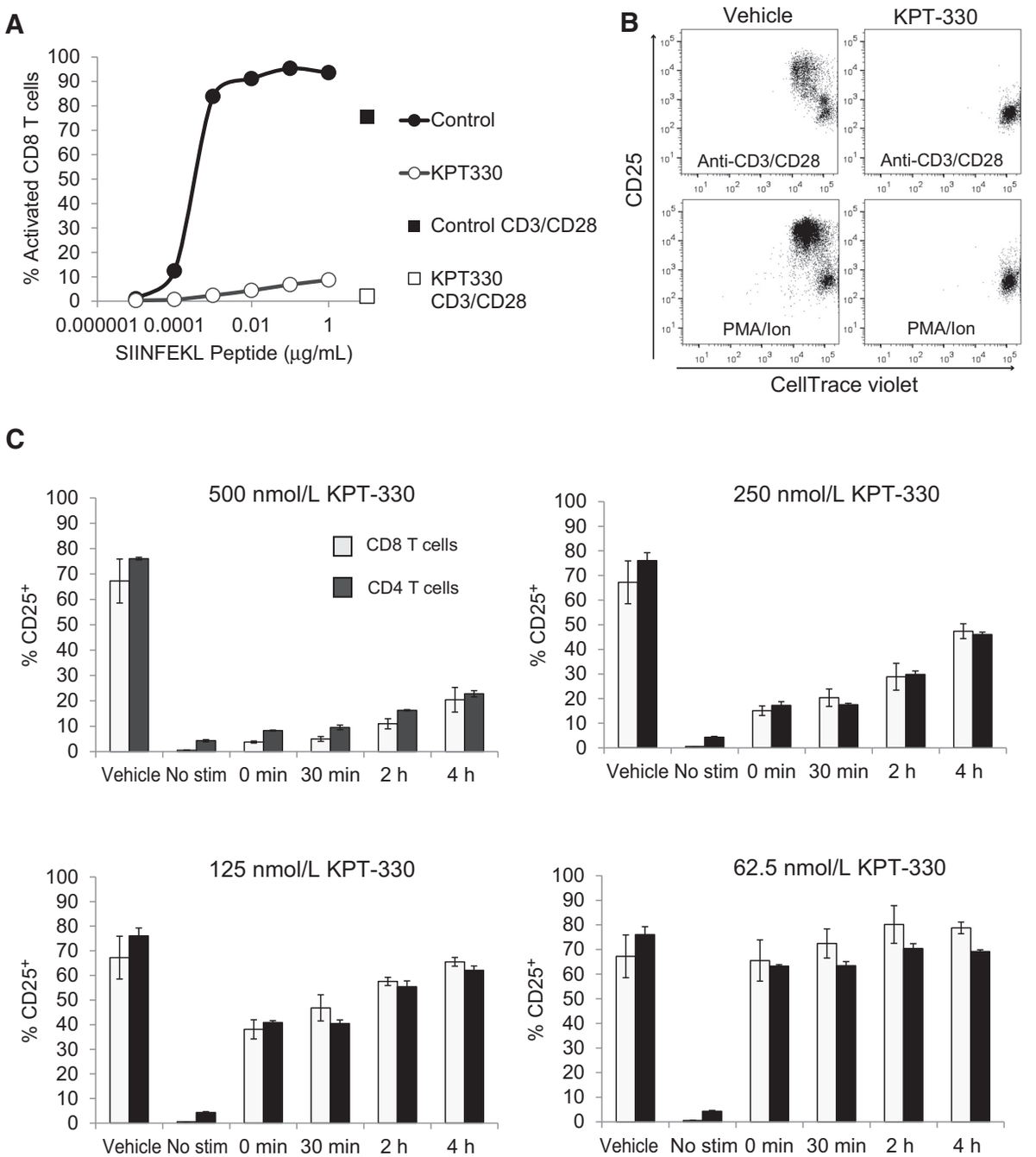

Figure 4.

Selinexor blocks activation of naïve T cells. **A,** CD8 T cells from an OT-I mouse were labeled with CellTrace violet and cocultured with CD40-activated B cells pulsed with ovalbumin peptide (SIINFEKL) at the indicated concentrations in the presence or absence of 1 μmol/L KPT-330. T-cell proliferation was measured by flow cytometry 3 days later. **B,** CD8 T cells from C57BL/6 mice were labeled with CellTrace violet and cocultured with anti-CD3/CD28–coated beads or PMA/Ion in the presence or absence of 1 μmol/L KPT-330. Three days later, cells were stained with anti-CD25 and anti-CD8 and analyzed by flow cytometry. **C,** Total lymph node cells from C57BL/6 mice were cultured with anti-CD3/CD28 beads and the indicated concentrations of KPT-330 added at the indicated time points relative to CD3/CD28 stimulation. Twenty-four hours later, cells were stained with antibodies to CD4, CD8, and CD25 and analyzed by flow cytometry.

TCR signaling involves a cascade of signaling molecules culminating in the translocation of activated NFAT, NF-κB, and AP-1 complexes into the nucleus. NFAT translocation occurs within minutes of TCR engagement; however, translocation of NF-κB and AP-1 complexes requires 2 to 4 hours (51, 52). Once the appropriate transcription factors had been

Published OnlineFirst February 1, 2017; DOI: 10.1158/1535-7163.MCT-16-0496

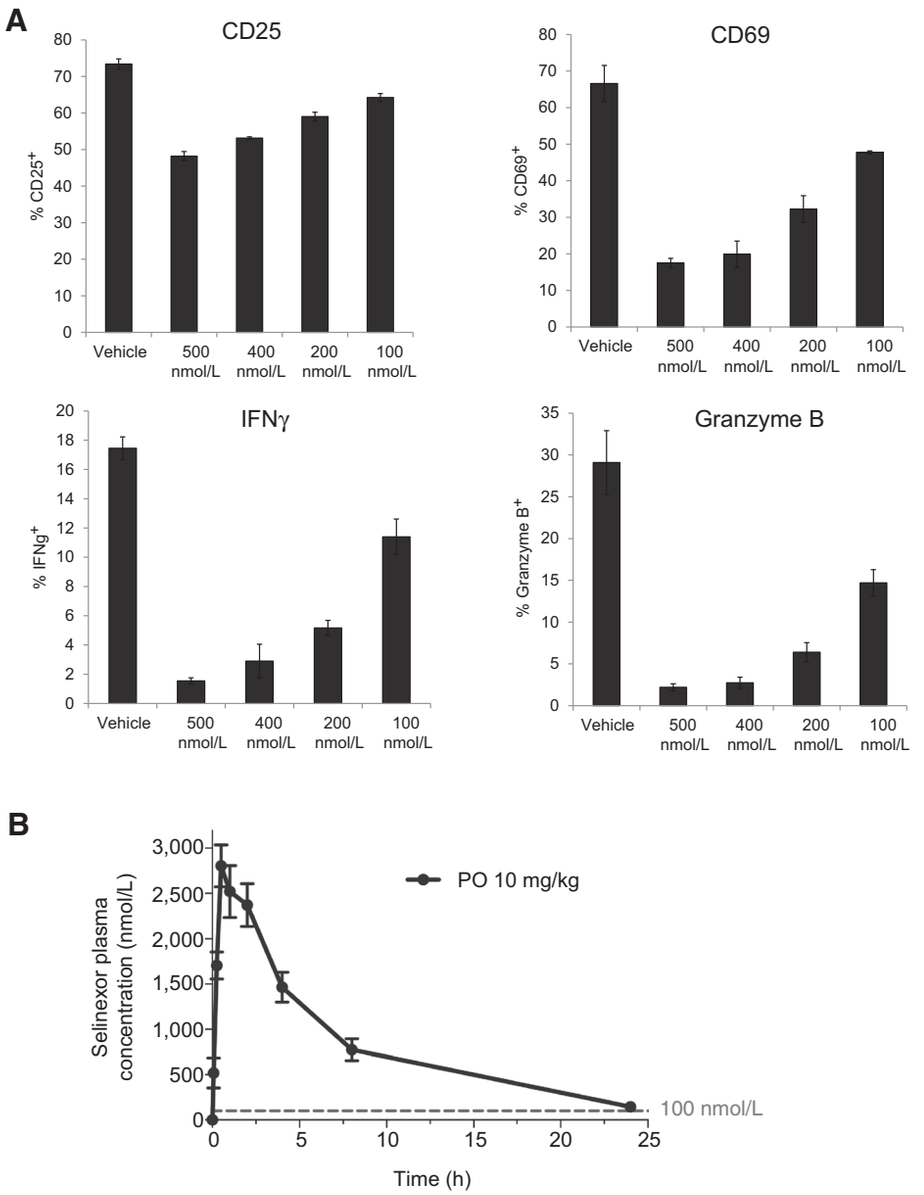

Figure 5.

Selinexor blocks the activation of effector CD8 T cells. **A,** CD8 T cells from an OT-I mouse were cultured with anti-CD3/CD28 beads for 7 days to generate effector cells. Effector cells were washed, counted, and plated onto B16OVA tumor cells that had been pretreated with IFNγ to induce MHC class I expression. KPT-330 was added to the cocultures at the indicated concentrations. Twenty-four hours later, OT-I cells were collected, fixed and permeabilized, and stained with antibodies to CD25, CD69, IFNγ, and granzyme B, and analyzed by flow cytometry. No response was seen from OT-I effector cells cultured with B16 cells not transduced with ovalbumin. Representative of three independent experiments. **B,** C57BL/6 mice were dosed with KPT-330 10 mg/kg by oral gavage. Serum was collected at various time points and analyzed for KPT-330 concentration by mass spectrometry. Dashed line, 100 nmol/L concentration.

shuttled into the nucleus, we predicted that T cells would be refractory to the inhibitory effects of selinexor. Indeed, both CD4 and CD8 T cells cultured with anti-CD3/CD28 beads in the presence of selinexor failed to become activated. However, this block in activation was lessened if selinexor was added to the cultures 4 hours after initial TCR engagement (Fig. 4C). Titration of both dose and time of addition revealed that naïve T cells were refractory to stimulation when selinexor was present within the first 4 hours after TCR engagement at concentrations greater than 100 nmol/L (Fig. 4D).

Selinexor blocks TCR signaling in effector T cells

Naïve T cells require signaling through both the TCR-associated CD3 complex, as well as through the costimulatory receptor CD28. Once primed, effector T cells become independent of CD28 signaling and will release effector cytokines and cytolytic molecules upon engagement with their cognate peptide–MHC on target cells. For cancer patients, intratumoral effector CD8 T cells are of particular interest, as this population is reinvigorated by anti-PD-1 checkpoint blockade therapy and is the key driver of antitumor immunity. We therefore investigated whether effector CD8 T cells were inhibited by selinexor. To generate effector cells *in vitro*, OT-I T cells were stimulated on anti-CD3/CD28 beads and cultured for 7 days. Effector cells were washed, counted, and cultured with B16 melanoma cells transduced with the model antigen ovalbumin (B16-OVA) in the presence of selinexor. After 24 hours of culture with target tumor cells, OT-I cells were analyzed for their upregulation of activation markers (CD25 and CD69) as well as expression of IFNγ and the cytolytic molecule granzyme B. Similar to naïve T cells, effector CD8 T-cell functions were blocked at concentrations of selinexor greater than 100 nmol/L (Fig. 5A; Supplementary Fig. S3).

Published OnlineFirst February 1, 2017; DOI: 10.1158/1535-7163.MCT-16-0496

We performed pharmacodynamics to determine the serum concentration of selinexor after oral dosing. Selinexor levels were greater than 100 nmol/L (44.3 ng/mL) for the first 24 hours post-oral dosing with 10 mg/kg (Fig. 5B). Similar kinetics have been observed in humans, with serum levels of selinexor dropping below 100 nmol/L after approximately 24 hours post-oral dosing (35 mg/m^2; ref. 17).

Optimized selinexor dosing does not inhibit antitumor immunity

The inhibitory effects of selinexor on CD8 T-cell function we observed *in vitro* were transient, and thus, we predicted that dose regimens of selinexor given with sufficient time intervals between dosing would allow for both normal immune homeostasis (Fig. 3) and the development of functional antitumor CD8 T cells. We inoculated mice subcutaneously with B16 melanoma, waited 6 to 7 days for the appearance of palpable tumors, and then began treating mice with 10 mg/kg selinexor on Monday and Wednesday, with a 4-day drug holiday incorporated into each weekly cycle. Tumor growth was significantly reduced in selinexor-treated mice (Fig. 6). After 2 weeks of treatment, tumors were harvested and tumor-infiltrating leukocyte (TIL) populations were analyzed. The total number of TILs was unaffected by selinexor treatment (Fig. 6A), and flow cytometric evaluation of various cell types of interest revealed no significant differences in CD4, CD8, natural killer (NK), B-cell, DC, or myeloid populations (Fig. 6B). Importantly, intratumoral CD8 T-cell numbers were unaffected.

We previously reported a mouse line cloned by somatic cell nuclear transfer from the nucleus of CD8 T cells specific for the melanoma antigen tyrosinase-related protein 1 (TRP1; ref. 48). The resulting TRP1 transnuclear mice have CD8 T cells specific for the endogenous antigen TRP1, which is highly expressed by B16 melanoma. To examine accumulation of tumor antigen–specific CD8 T cells, we stimulated TRP1^{high};CD45.1$^+$ CD8 T cells *in vitro* and transferred these activated TRP1-specific T cells into mice bearing day 12 B16 tumors (48). We then used expression of the congenic marker CD45.1 to measure accumulation of antigen-specific CD8 T cells, expression of various activation and exhaustion markers, as well as expression of IFNγ and granzyme B. We observed very little effect of selinexor on any of these parameters in antigen-specific TRP1 cells (Fig. 6C) or endogenous CD8 T cells (Fig. 6D). PD-1, LAG3, and CD44 were reduced on TRP1 cells from KPT-330–treated mice, with a similar trend in endogenous CD8 T cells, suggesting slightly decreased T-cell activation. Importantly, no differences were observed in intracellular IFNγ or granzyme B, indicating that CD8 T-cell effector functions are preserved.

The most commonly used checkpoint blockade drugs today block the PD-1:PD-L1 signaling pathway. Selinexor treatment neither affected PD-1 expression on intratumoral CD8 T cells nor the expression of PD-L1 on B16 tumor cells or tumor-infiltrating myeloid populations (Fig. 6D). Therefore, combination of PD-1:PD-L1 blockade with selinexor would be predicted to have added benefit over selinexor treatment alone, as indeed was observed by Farren and colleagues (cosubmitted with this article).

Discussion

Selinexor alters the nuclear localization of some 200 proteins that rely on XPO1 for export from the nucleus. Several of these XPO1 cargos are absolutely required for immune cell development and function. We found that T cells, most notably CD8 T cells, were sensitive to selinexor treatment. *In vivo*, selinexor dosing caused dramatic reductions in thymocyte numbers and a progressive loss of CD8 T cells from bone marrow, spleen, and lymph nodes. Naïve CD4 and CD8 T cells were refractory to activation in the presence of selinexor. Effector CD8 T cells, despite no longer requiring costimulation, were also blocked in their capacity to degranulate or produce IFNγ when selinexor was present. Although we do not identify the exact proteins whose improper nuclear localization causes these effects on T cells, we suspect that several players contribute, including NF-κB, a heterodimeric transcription factor that is sequestered in the nucleus with its inhibitor IκBα upon blockade of XPO1 (28). Mice that overexpress IκBα show perturbations in thymic development and a loss of CD8 T cells from the spleen and lymph nodes (53), similar to the effects we observe in selinexor-treated mice. Together, these findings suggest that nuclear exportins are required for T-cell development and function.

T cells require signaling through their TCRs at several distinct stages. During development in the thymus, CD4$^+$CD8$^+$ (DP) T cells encounter self-peptides presented on MHC class I and MHC class II molecules. In a process of positive and negative selection, T cells that are overtly self-reactive are deleted, while T cells that fail to recognize self-MHC molecules also undergo apoptosis. Intermediate levels of TCR signaling are required for CD4 and CD8 T cells to survive thymic selection and emigrate to the spleen and lymph nodes as so called naïve T cells. Naïve T cells require TCR signaling again upon initial encounter with antigen, usually on a dendritic cell. Activation of naïve T cells leads to proliferation, trafficking from the lymph nodes to tissues, and acquisition of effector functions, such as cytokine production and development of cytolytic granules. Upon reaching the inflamed tissue, effector T cells require TCR signaling via contact with peptide–MHC to correctly identify and kill their target cells.

Of the three steps at which selinexor might block CD8 T-cell development and function, the effector stage is potentially the most concerning. Effector CD8 T cells are present in many human tumors, and PD-1 blockade therapies operate by reactivating this population (54, 55). If selinexor is to be used safely in humans, particularly in combination with anti-PD-1 mAbs, we wanted to first determine whether the intratumoral effector CD8 T cells were still functional in selinexor-treated mouse models. We first administered selinexor at 15 mg/kg dosed 3 times per week starting at the time of tumor inoculation. At this very frequent dosing schedule, we found nearly undetectable levels of CD8 T cells in the tumors and were therefore unable to assess their function (data not shown). However, when we decreased the dosing frequency to 10 mg/kg given Monday and Wednesday with a 4-day drug holiday each week, this optimized dosing cycle allowed for robust CD8 T-cell infiltrates. We carefully assessed activation markers, IFNγ production, development of cytolytic granules, and accumulation of antigen-specific CD8 T cells and found that in all respects, the CD8 T-cell immune response appeared normal. We also found normal levels of CD4 T cells, Tregs, NK cells, dendritic cells, macrophages, and MDSCs. PD-L1 surface expression was likewise unchanged. The recommended phase II dosing regimen of selinexor is 60 mg (35.3 mg/m^2) given twice weekly (days 1 and 3; ref. 17). This dosing is supported by the optimized dosing regimen that we propose here for the maintenance of antitumor immunity. In a report cosubmitted with our article, Farren and colleagues examined combination of selinexor with checkpoint blockade in

Published OnlineFirst February 1, 2017; DOI: 10.1158/1535-7163.MCT-16-0496

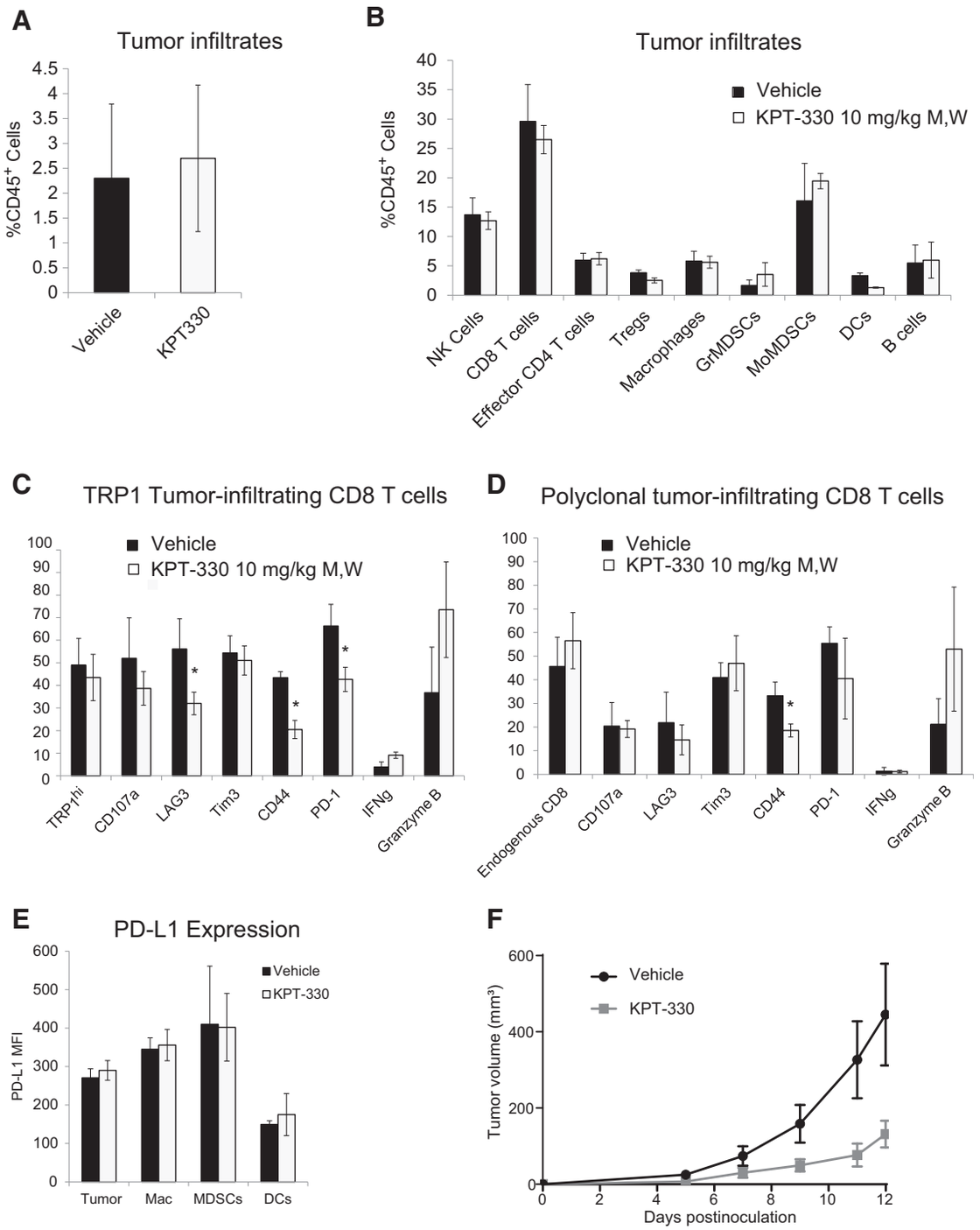

Figure 6.

Optimized selinexor dosing does not inhibit antitumor immunity *in vivo*. **A,** C57BL/6 mice were inoculated subcutaneously with 1×10^5 B16 cells on day 0. On days 7, 9, 14, and 16, mice were dosed with vehicle or 10 mg/kg KPT-330 by oral gavage. Tumors were harvested on day 21, digested and infiltrates analyzed by flow cytometry. Total $CD45^+$ cells were quantified. $n = 5$ mice per group. Representative of two experiments. **B,** Tumor infiltrates from **A** were stained with antibodies to CD45, CD8, CD4, NK1.1, B220, MHC class II, Gr1, Foxp3, CD11b, and CD11c and analyzed by flow cytometry. $n = 5$ mice per group. Representative of two experiments. M, Monday; W, Wednesday. **C,** C57BL/6 mice were inoculated with B16 tumors and dosed with 10 mg/kg KPT-330 on days 6, 8, 13, and 15. On day 12 after tumor inoculation, all mice received adoptive transfer of 5×10^5 activated $TRP1^{high}$;$CD45.1^+$ CD8 T cells. On day 17, tumor infiltrates were harvested, stained with the indicated antibodies, and analyzed by flow cytometry after gating on $CD45^+CD8^+CD45.1^+$ TRP1-specific cells. $n = 5$ mice per group. **D,** Tumor infiltrates from **C** were gated on endogenous CD8 T cells ($CD45^+CD8^+CD45.1^-$). **E,** Tumor infiltrates from **C** were stained with antibodies to PD-L1 and other cell surface markers. Mean fluorescence intensity (MFI) of PD-L1 expression was quantified. Tumor = $CD45^-$; Mac = $CD45^+CD11b^+Gr1^-CD11c^-$; MDSCs = $CD45^+CD11b^+Gr1^+$; dendritic cells = $CD45^+MHCII^+CD11c^+$. $n = 5$ mice per group. **F,** Tumor growth of mice analyzed in **C** and **D**.

Published OnlineFirst February 1, 2017; DOI: 10.1158/1535-7163.MCT-16-0496

mice and found that selinexor dosing twice weekly enhances the efficacy of PD-1 blockade, whereas daily dosing has no effect. Together, our studies support the initiation of clinical trials of selinexor and PD-1 blockade, using the optimized twice weekly dosing of selinexor (days 1 and 3).

Combination immune therapies are becoming increasingly common as more chemotherapies and targeted drugs are being paired with immunotherapy agents. Many chemotherapeutics kill rapidly dividing cells, which includes cells of the immune system (44). Effector CD8 T cells could easily be collateral damage in many combination regimens. Here, we show that twice weekly (but not daily) dosing of selinexor dosing allows sufficient time for a fully functional antitumor CD8 T-cell response. These results argue for a careful assessment of scheduling when designing combination regimens of small molecules with immunotherapy agents, which in many cases can be done rapidly in preclinical mouse models.

Disclosure of Potential Conflicts of Interest

B. Klebanov, T. Kashyap, S. Sacham, and Y. Landesman are employees of Karyopharm Therapeutics. S.K. Dougan was funded by a sponsored research agreement with Karyopharm Therapeutics. No potential conflicts of interest were disclosed by the other authors.

Authors' Contributions

Conception and design: P.M. Tyler, M.M. Servos, S. Sacham, S.K. Dougan
Development of methodology: P.M. Tyler, M.M. Servos, T. Kashyap, M. Dougan, S.K. Dougan
Acquisition of data (provided animals, acquired and managed patients, provided facilities, etc.): P.M. Tyler, M.M. Servos, R.C. de Vries, S.K. Dougan
Analysis and interpretation of data (e.g., statistical analysis, biostatistics, computational analysis): P.M. Tyler, M.M. Servos, R.C. de Vries, M. Dougan, S.K. Dougan
Writing, review, and/or revision of the manuscript: P.M. Tyler, M.M. Servos, B. Klebanov, S. Sacham, Y. Landesman, M. Dougan, S.K. Dougan
Administrative, technical, or material support (i.e., reporting or organizing data, constructing databases): P.M. Tyler, M.M. Servos, R.C. de Vries, B. Klebanov

Acknowledgments

We are grateful to James Maiarana for maintaining the flow cytometer.

Grant Support

S.K. Dougan was funded by a sponsored research agreement with Karyopharm Therapeutics, as well as by the Claudia Adams Barr Foundation and the Melanoma Research Alliance. M. Dougan was supported by an NIH Ruth L. Kirschstein National Research Service Award (1F32CA210568-01).

The costs of publication of this article were defrayed in part by the payment of page charges. This article must therefore be hereby marked *advertisement* in accordance with 18 U.S.C. Section 1734 solely to indicate this fact.

Received July 28, 2016; revised December 3, 2016; accepted December 27, 2016; published OnlineFirst February 1, 2017.

References

1. Zaidi SK, Young DW, Javed A, Pratap J, Montecino M, van Wijnen A, et al. Nuclear microenvironments in biological control and cancer. Nat Rev Cancer 2007;7:454–63.
2. Turner JG, Dawson J, Sullivan DM. Nuclear export of proteins and drug resistance in cancer. Biochem Pharmacol 2012;83:1021–32.
3. Mahipal A, Malafa M. Importins and exportins as therapeutic targets in cancer. Pharmacol Ther 2016;164:135–43.
4. Fukuda M, Asano S, Nakamura T, Adachi M, Yoshida M, Yanagida M, et al. CRM1 is responsible for intracellular transport mediated by the nuclear export signal. Nature 1997;390:308–11.
5. Ossareh-Nazari B, Bachelerie F, Dargemont C. Evidence for a role of CRM1 in signal-mediated nuclear protein export. Science 1997;278:141–4.
6. Xu D, Grishin NV, Chook YM. NESdb: a database of NES-containing CRM1 cargoes. Mol Biol Cell 2012;23:3673–6.
7. Tan DS, Bedard PL, Kuruvilla J, Siu LL, Razak AR. Promising SINEs for embargoing nuclear-cytoplasmic export as an anticancer strategy. Cancer Discov 2014;4:527–37.
8. Noske A, Weichert W, Niesporek S, Roske A, Buckendahl AC, Koch I, et al. Expression of the nuclear export protein chromosomal region maintenance/exportin 1/Xpo1 is a prognostic factor in human ovarian cancer. Cancer 2008;112:1733–43.
9. Huang WY, Yue L, Qiu WS, Wang LW, Zhou XH, Sun YJ. Prognostic value of CRM1 in pancreas cancer. Clin Invest Med 2009;32:E315.
10. Shen A, Wang Y, Zhao Y, Zou L, Sun L, Cheng C. Expression of CRM1 in human gliomas and its significance in p27 expression and clinical prognosis. Neurosurgery 2009;65:153–9.
11. van der Watt PJ, Maske CP, Hendricks DT, Parker MI, Denny L, Govender D, et al. The Karyopherin proteins, Crm1 and Karyopherin beta1, are overexpressed in cervical cancer and are critical for cancer cell survival and proliferation. Int J Cancer 2009;124:1829–40.
12. van der Watt PJ, Leaner VD. The nuclear exporter, Crm1, is regulated by NFY and Sp1 in cancer cells and repressed by p53 in response to DNA damage. Biochim Biophys Acta 2011;1809:316–26.
13. Zhou F, Qiu W, Yao R, Xiang J, Sun X, Liu S, et al. CRM1 is a novel independent prognostic factor for the poor prognosis of gastric carcinomas. Med Oncol 2013;30:726
14. Yao Y, Dong Y, Lin F, Zhao H, Shen Z, Chen P, et al. The expression of CRM1 is associated with prognosis in human osteosarcoma. Oncol Rep 2009;21:229–35.
15. Salas Fragomeni RA, Chung HW, Landesman Y, Senapedis W, Saint-Martin JR, Tsao H, et al. CRM1 and BRAF inhibition synergize and induce tumor regression in BRAF-mutant melanoma. Mol Cancer Ther 2013;12:1171–9.
16. Senapedis WT, Baloglu E, Landesman Y. Clinical translation of nuclear export inhibitors in cancer. Semin Cancer Biol 2014;27:74–86.
17. Abdul Razak AR, Mau-Soerensen M, Gabrail NY, Gerecitano JF, Shields AF, Unger TJ, et al. First-in-class, first-in-human phase I study of selinexor, a selective inhibitor of nuclear export, in patients with advanced solid tumors. J Clin Oncol 2016;34:4142–50.
18. Etchin J, Montero J, Berezovskaya A, Le BT, Kentsis A, Christie AL, et al. Activity of a selective inhibitor of nuclear export, selinexor (KPT-330), against AML-initiating cells engrafted into immunosuppressed NSG mice. Leukemia 2016;30:190–9.
19. De Cesare M, Cominetti D, Doldi V, Lopergolo A, Deraco M, Gandellini P, et al. Anti-tumor activity of selective inhibitors of XPO1/CRM1-mediated nuclear export in diffuse malignant peritoneal mesothelioma: the role of survivin. Oncotarget 2015;6:13119–32.
20. Hing ZA, Mantel R, Beckwith KA, Guinn D, Williams E, Smith LL, et al. Selinexor is effective in acquired resistance to ibrutinib and synergizes with ibrutinib in chronic lymphocytic leukemia. Blood 2015;125:3128–32.
21. Yang J, Bill MA, Young GS, La Perle K, Landesman Y, Shacham S, et al. Novel small molecule XPO1/CRM1 inhibitors induce nuclear accumulation of TP53, phosphorylated MAPK and apoptosis in human melanoma cells. PLoS One 2014;9:e102983.
22. Ranganathan P, Kashyap T, Yu X, Meng X, Lai TH, McNeil B, et al. XPO1 inhibition using selinexor synergizes with chemotherapy in acute myeloid leukemia (AML) by targeting DNA repair and restoring topoisomerase IIα to the nucleus. Clin Cancer Res 2016;22:6142–52.
23. Ranganathan P, Yu X, Santhanam R, Hofstetter J, Walker A, Walsh K, et al. Decitabine priming enhances the antileukemic effects of exportin 1 (XPO1) selective inhibitor selinexor in acute myeloid leukemia. Blood 2015;125:2689–92.

24. Begitt A, Meyer T, van Rossum M, Vinkemeier U. Nucleocytoplasmic translocation of Stat1 is regulated by a leucine-rich export signal in the coiled-coil domain. Proc Natl Acad Sci U S A 2000;97:10418–23.
25. Bhattacharya S, Schindler C. Regulation of Stat3 nuclear export. J Clin Invest 2003;111:553–9.
26. Tai YT, Landesman Y, Acharya C, Calle Y, Zhong MY, Cea M, et al. CRM1 inhibition induces tumor cell cytotoxicity and impairs osteoclastogenesis in multiple myeloma: molecular mechanisms and therapeutic implications. Leukemia 2014;28:155–65.
27. Huang TT, Kudo N, Yoshida M, Miyamoto S. A nuclear export signal in the N-terminal regulatory domain of IkappaBalpha controls cytoplasmic localization of inactive NF-kappaB/IkappaBalpha complexes. Proc Natl Acad Sci U S A 2000;97:1014–9.
28. Kashyap T, Argueta C, Aboukameel A, Unger TJ, Klebanov B, Mohammad RM, et al. Selinexor, a Selective Inhibitor of Nuclear Export (SINE) compound, acts through NF-κB deactivation and combines with proteasome inhibitors to synergistically induce tumor cell death. Oncotarget 2016; 7:78883–95.
29. Galon J, Costes A, Sanchez-Cabo F, Kirilovsky A, Mlecnik B, Lagorce-Pages C, et al. Type, density, and location of immune cells within human colorectal tumors predict clinical outcome. Science 2006;313:1960–4.
30. Postow MA, Chesney J, Pavlick AC, Robert C, Grossmann K, McDermott D, et al. Nivolumab and ipilimumab versus ipilimumab in untreated melanoma. N Engl J Med 2015;372:2006–17.
31. Topalian SL, Hodi FS, Brahmer JR, Gettinger SN, Smith DC, McDermott DF, et al. Safety, activity, and immune correlates of anti-PD-1 antibody in cancer. N Engl J Med 2012;366:2443–54.
32. Hodi FS, O'Day SJ, McDermott DF, Weber RW, Sosman JA, Haanen JB,et al. Improved survival with ipilimumab in patients with metastatic melanoma. N Engl J Med 2010;363:711–23.
33. Wolchok JD, Kluger H, Callahan MK, Postow MA, Rizvi NA, Lesokhin AM, et al. Nivolumab plus ipilimumab in advanced melanoma. N Engl J Med 2013;369:122–33.
34. Ansell SM, Lesokhin AM, Borrello I, Halwani A, Scott EC, Gutierrez M, et al. PD-1 blockade with nivolumab in relapsed or refractory Hodgkin's lymphoma. N Engl J Med 2015;372:311–9.
35. Le DT, Uram JN, Wang H, Bartlett BR, Kemberling H, Eyring AD, et al. PD-1 blockade in tumors with mismatch-repair deficiency. N Engl J Med 2015;372:2509–20.
36. Pfirschke C, Engblom C, Rickelt S, Cortez-Retamozo V, Garris C, Pucci F, et al. Immunogenic chemotherapy sensitizes tumors to checkpoint blockade therapy. Immunity 2016;44:343–54.
37. Galluzzi L, Buque A, Kepp O, Zitvogel L, Kroemer G. Immunological effects of conventional chemotherapy and targeted anticancer agents. Cancer Cell 2015;28:690–714.
38. Postow MA, Callahan MK, Barker CA, Yamada Y, Yuan J, Kitano S, et al. Immunologic correlates of the abscopal effect in a patient with melanoma. N Engl J Med 2015;366:925–31.
39. Twyman-Saint Victor C, Rech AJ, Maity A, Rengan R, Pauken KE, Stelekati E, et al. Radiation and dual checkpoint blockade activate non-redundant immune mechanisms in cancer. Nature 2015;520:373–7.
40. Winograd R, Byrne KT, Evans RA, Odorizzi PM, Meyer AR, Bajor DL, et al. Induction of T-cell immunity overcomes complete resistance to PD-1 and CTLA-4 Blockade and improves survival in pancreatic carcinoma. Cancer Immunol Res 2015;3:399–411.
41. Boni A, Cogdill AP, Dang P, Udayakumar D, Njauw CN, Sloss CM, et al. Selective BRAFV600E inhibition enhances T-cell recognition of melanoma without affecting lymphocyte function. Cancer Res 2010;70:5213–9.
42. Wyluda EJ, Cheng J, Schell TD, Haley JS, Mallon C, Neves RI, et al. Durable complete responses off all treatment in patients with metastatic malignant melanoma after sequential immunotherapy followed by a finite course of BRAF inhibitor therapy. Cancer Biol Ther 2015;16:662–70.
43. Wang HH, Cui YL, Zaorsky NG, Lan J, Deng L, Zeng XL, et al. Mesenchymal stem cells generate pericytes to promote tumor recurrence via vasculogenesis after stereotactic body radiation therapy. Cancer Lett 2016;375:349–59.
44. Apetoh L, Ladoire S, Coukos G, Ghiringhelli F. Combining immunotherapy and anticancer agents: the right path to achieve cancer cure? Ann Oncol 2015;26:1813–23.
45. Suzuki E, Kapoor V, Jassar AS, Kaiser LR, Albelda SM. Gemcitabine selectively eliminates splenic Gr-1+/CD11b+ myeloid suppressor cells in tumor-bearing animals and enhances antitumor immune activity. Clin Cancer Res 2005;11:6713–21.
46. Vincent J, Mignot G, Chalmin F, Ladoire S, Bruchard M, Chevriaux A, et al. 5-Fluorouracil selectively kills tumor-associated myeloid-derived suppressor cells resulting in enhanced T cell-dependent antitumor immunity. Cancer Res 2010;70:3052–61.
47. Bauer C, Sterzik A, Bauernfeind F, Duewell P, Conrad C, Kiefl R, et al. Concomitant gemcitabine therapy negatively affects DC vaccine-induced CD8(+) T-cell and B-cell responses but improves clinical efficacy in a murine pancreatic carcinoma model. Cancer Immunol Immunother 2014;63:321–33.
48. Dougan SK, Dougan M, Kim J, Turner JA, Ogata S, Cho HI, et al. Transnuclear TRP1-specific CD8 T cells with high or low affinity TCRs show equivalent antitumor activity. Cancer Immunol Res 2013;1:99–111.
49. Morris GP, Allen PM. How the TCR balances sensitivity and specificity for the recognition of self and pathogens. Nat Immunol 2012;13:121–8.
50. Hogquist KA, Jameson SC, Heath WR, Howard JL, Bevan MJ, Carbone FR. T cell receptor antagonist peptides induce positive selection. Cell 1994;76:17–27.
51. Huang YH, Sojka DK, Fowell DJ. Cutting edge: regulatory T cells selectively attenuate, not terminate, T cell signaling by disrupting NF-kappaB nuclear accumulation in CD4 T cells. J Immunol 2012;188:947–51.
52. Marangoni F, Murooka TT, Manzo T, Kim EY, Carrizosa E, Elpek NM, et al. The transcription factor NFAT exhibits signal memory during serial T cell interactions with antigen-presenting cells. Immunity 2013;38: 237–49.
53. Boothby MR, Mora AL, Scherer DC, Brockman JA, Ballard DW. Perturbation of the T lymphocyte lineage in transgenic mice expressing a constitutive repressor of nuclear factor (NF)-kappaB. J Exp Med 1997;185:1897–907.
54. Spranger S, Koblish HK, Horton B, Scherle PA, Newton R, Gajewski TF. Mechanism of tumor rejection with doublets of CTLA-4, PD-1/PD-L1, or IDO blockade involves restored IL-2 production and proliferation of CD8 (+) T cells directly within the tumor microenvironment. J Immunother Cancer 2014;2:3.
55. Curran MA, Montalvo W, Yagita H, Allison JP. PD-1 and CTLA-4 combination blockade expands infiltrating T cells and reduces regulatory T and myeloid cells within B16 melanoma tumors. Proc Natl Acad Sci U S A 2010;107:4275–80.

Published OnlineFirst February 1, 2017; DOI: 10.1158/1535-7163.MCT-16-0496

Molecular Cancer Therapeutics

Clinical Dosing Regimen of Selinexor Maintains Normal Immune Homeostasis and T-cell Effector Function in Mice: Implications for Combination with Immunotherapy

Paul M. Tyler, Mariah M. Servos, Romy C. de Vries, et al.

Mol Cancer Ther 2017;16:428-439. Published OnlineFirst February 1, 2017.